I&EC research
Industrial & Engineering Chemistry Research

Article

pubs.acs.org/IECR

Multiphase Equilibria Modeling with GCA-EoS. Part I: Carbon Dioxide with the Homologous Series of Alkanes up to 36 Carbons

Mariana González Prieto, Francisco Adrián Sánchez, and Selva Pereda*

Planta Piloto de Ingeniería Química (PLAPIQUI), CONICET, Universidad Nacional del Sur (UNS), Camino La Carrindanga Km 7, CC 717, Bahía Blanca 8000, Argentina

ABSTRACT: The Group Contribution with Association Equation of State (GCA-EoS) has been successfully applied to represent the global phase behavior of carbon dioxide mixtures with alkanes. Using a single set of parameters, the model is able to predict vapor−liquid and liquid−liquid equilibria of binary mixtures not included in the parametrization procedure. Special emphasis was set on describing the transformation between types of fluid phase behavior to reduce the jeopardy of predicting incorrect liquid split. This family of binary systems has been investigated in previous works; however, this is the first time that GCA-EoS was shown to be able to represent the transformation between types of phase behavior as the length of the alkyl chain increases. The model was tested against an experimental database covering C_3−C_{36} alkanes, temperatures from 210 to 660 K, and pressures up to 400 bar. The wide range of conditions and the parametrization strategy are keys to develop a robust thermodynamic tool for predicting multiphase behavior.

1. INTRODUCTION

Modeling phase equilibria in mixtures containing alkanes and carbon dioxide (CO_2) is a challenge for any equation of state. The task is even more complex for a group contribution method, which uses a single set of interaction parameters for all the binaries of the homologous series. The nonideality highly affects the behavior of these mixtures, causing multiple transformations between types of phase behavior as the alkyl chain increases, namely, the binary mixtures of CO_2 show phase behavior Type II with alkanes up to *n*-undecane, Type IV with *n*-tridecane, and Type III with higher alkanes, according to the van Konynenburg and Scott[1] classification. Briefly, Type II presents a continuous critical L = V locus bounded between the pure components critical points. In addition, these systems show liquid immiscibility at low temperature, which generates the appearance of a second critical line (L1 = L2), also known as upper critical solution temperatures (UCST points) starting from the three-phase equilibrium line L1L2V as can be seen in Figure 1a. In the *PT* projection, the intersection of the L1 = L2 critical line with the L1L2V line corresponds to an upper critical end point (UCEP of the class L1 = L2V). In Figure 1a, we sketched the critical line L1 = L2 with a positive slope, but it can also be negative or show a maximum or minimum in temperature. In many cases solid phase formation hinders the potential for low-temperature liquid split. If this is the case, from a practical point of view we will not be able to distinguish between Type I (completely miscible systems) and Type II phase behavior. For example, the binary systems CO_2 + *n*-alkanes with 6−12 carbons show Type II phase behavior, but with pentane the liquid immiscibility is inhibited by the CO_2 precipitation.[2] On the other hand, when the liquid immiscibility interrupts the L = V critical curve, it leads to Type III behavior (see Figure 1b). The main trait of this case is the existence of liquid immiscibility from low temperatures up to the end of light component existence as a liquid, nearby its critical point (CP). The L1 = V critical line starting from this CP stretches out up to the L1L2V equilibrium line in a UCEP; in general, this critical line is short because the L1L2V line usually runs close to the more volatile component vapor pressure curve. This fact means that the UCEP, as a rule, is located close to the light component CP. Furthermore, the greater the difference of volatility between both components, the L1L2V curve gets even closer to the light component vapor pressure curve. The L2 = V critical line starting from the heavier compound CP will diverge toward high pressures. Finally, Type IV (Figure 1c) phase behavior is quite unusual; it shows liquid phase split at low and high temperature, but the mixture becomes completely miscible at an intermediate temperature range. Consequently, the system shows a low-temperature L1 = L2 critical univariant line that diverges toward high pressures and a discontinuous L = V critical line. In addition, Type IV phase behavior shows two UCEP and one LCEP due to the discontinuity of the three-phase L1L2V equilibrium. Figure 1 also shows the typical temperature−composition projection of each type of phase behavior depicted by CO_2 + *n*-alkane mixtures.

Several authors[3−10] have correlated isolated binary systems of this homologous series using either isobaric or isothermal data sets. This approach can lead to wrong predictions outside the range of the correlated experimental data because it may fail to notice the comprehensive phase behavior of these mixtures. In this regard, it is common to find models showing liquid split for completely miscible systems.[6,7] Parameterization of a model taking into account the transformation of type of phase behavior as the alkane chain grows is not a simple work. Nevertheless, some authors[11−17] recognized the importance of considering the comprehensive phase behavior and made efforts to model the phase transition using either transferable parameters (i.e., the same parameters for all binary interactions

Received: September 3, 2015
Revised: October 20, 2015
Accepted: November 17, 2015
Published: November 17, 2015

DOI: 10.1021/acs.iecr.5b03269
Ind. Eng. Chem. Res. 2015, 54, 12415−12427

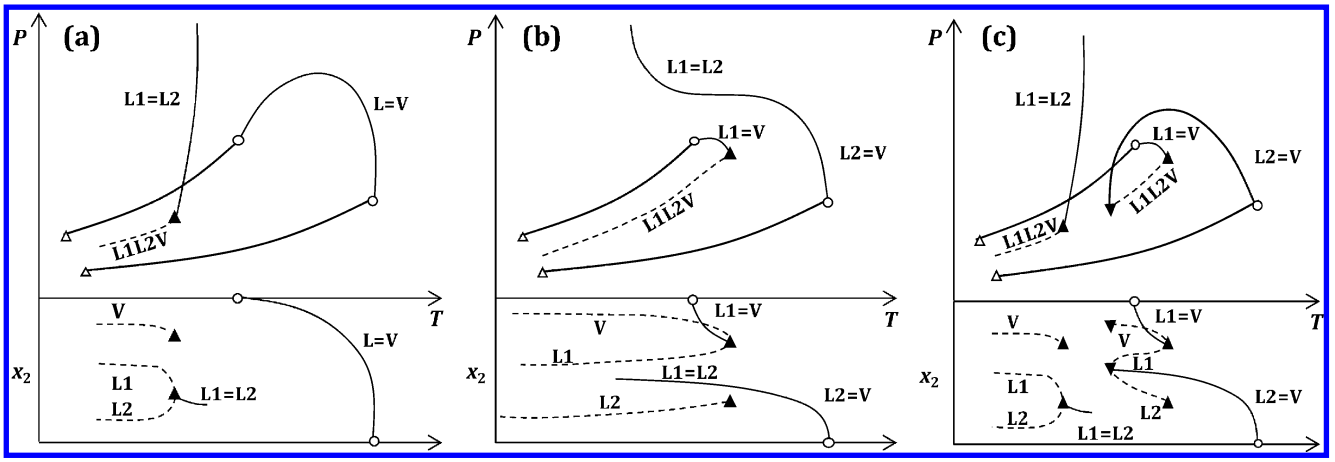

Figure 1. Types of fluid phase behavior depicted by CO_2 + *n*-alkane binary homologous series according to the van Konynenburg and Scott[1] classification. (a) Type II, (b) Type III, and (c) Type IV.

of the homologous series), generalized correlations of binary parameters, or a group contribution approach. In this regard, Polishuk et al.[12,13] proposed fitting the binary interaction parameters of a cubic equation of state to the UCEP and critical pressure maximum. Using C4EoS with quadratic mixing rules, they were able to model correctly the transformation between types of fluid phase behavior and qualitatively the mutual solubility between CO_2 and *n*-alkanes. On the other hand, Cismondi et al.[14] also considered the correlation of the interaction parameters to key equilibrium points of some binary mixtures, comprising critical points, VLE, and LLE experimental data. In this case, the authors applied RKPR-EoS with cubic mixing rules (CMR) for the mixture parameters. The CMR involve eight binary interaction parameters, which in this case were correlated with a fourth-order polynomial expression as a function of the carbon number. This flexible mixing rule allows achieving accurate predictions in the complete *PVTx* space for the CO_2 + *n*-alkane homologous series.

Alternatively, some authors used thermodynamic perturbation theory based equations of state taking into account the type of phase behavior during the parametrization. Galindo and Blas,[15] García et al,[16] and Llovell and Vega[17] applied, respectively, the SAFT-VR, PC-SAFT, and Soft-SAFT EoS to investigate the CO_2 + *n*-alkane homologous series. The three groups followed a similar approach: they correlated the interaction parameter (two in the case of Galindo and Blas) to represent the binary mixture of CO_2 + *n*-tridecane, which is the only binary system of the homologous series that shows Type IV phase behavior. Then they predicted the phase behavior of the other binaries of the homologous series transferring the interaction parameter. The models depicted qualitatively correct predictions in most of the cases. Galindo and Blas[15] and Llovell and Vega[17] also showed precise *PT* projections of the critical loci.

All previously discussed contributions applied molecular models, which show limited capabilities to predict, with high accuracy, other binaries than those that were correlated. It is important to bear in mind that the systems under study show a significant change of phase behavior as the alkyl chain increases. Therefore, hardly a molecular model can achieve accurate predictions by means of transferring parameters. Particularly, group contribution methods are a well-suited approach when dealing with multicomponent mixtures containing compounds with similar structures. As benefits, not only potential accurate predictions can be achieved but also the number of required binary interaction parameters is greatly reduced. For instance, Horstmann et al.[8] applied the PSRK model to correlate the vapor−liquid critical locus of CO_2 + ethane. Subsequently, they showed accurate predictions of CO_2 + *n*-butane VLE data and Henry constants of CO_2 in *n*-hexadecane using the same parameters. Moreover, Vitu et al.[9] performed an extensive thermodynamic modeling with PPR78 of CO_2 + hydrocarbons (methane up to *n*-nonadecane) mixtures. They achieved good results in VLE and critical loci calculation of several binary systems. On the other hand, Nguyen-Huynh[10] used the GC-PPC-SAFT EoS to model the phase equilibria of CO_2 + *n*-alkanes up to *n*-tetratetracontane. The authors correlated the VLE of some CO_2 + *n*-alkane binary systems and were able to accurately predict the VLE of other investigated binaries. In all these cases, isolated binary VLE data was correlated and nothing was discussed regarding the LLE and the transformation between types of phase behavior.

The aim of this work is to show a parametrization strategy with focus on the quantitative representation of the binary mixture phase equilibria without compromising the prediction of the global phase behavior and its transformation within the homologous family. We investigate the correlation and prediction of CO_2 + alkane binary mixtures using a group contribution approach and including the *PTx* projections of CO_2 with alkanes from propane up to *n*-hexatriacontane and their excess properties when available. Furthermore, we also challenged the model to predict binary systems of CO_2 + branched alkanes with the same set of parameters. This review of alkyl chains parametrization will also provide a basis to improve the modeling of other homologous series with CO_2 such as alcohols, ethers, carboxylic acids, etc.

2. THERMODYNAMIC MODELING

A robust parametrization of a group contribution model compels one to consider the transformation between types of phase behavior as the alkyl chain grows. Given this somehow evident statement, it is not always easy to be considered because the behavior of the whole series must be described with the same set of binary interaction parameters by only changing the number of functional groups. In this work we review the modeling of the CO_2 + *n*-alkanes series phase behavior using the Group Contribution with Association Equation of State (GCA-EoS).[18] Previous works have shown the capacity of this model to accurately represent the complex multiphase behavior of mixtures containing

DOI: 10.1021/acs.iecr.5b03269
Ind. Eng. Chem. Res. 2015, 54, 12415−12427

hydrocarbons with polar and associating compounds, such as alcohols and water,[19−22] amines,[23,24] and furans.[25] Moreover, this model also showed excellent predictive potential when applied to the phase behavior of multicomponent mixtures containing natural products[26−31] or fuel blends.[32−34] It is worth mentioning that the GCA-EoS is an extension to associating mixtures of the GC-EoS, originally proposed by Skjold-Jørgensen[35] to model gas solubility. Therefore, parameters for nonassociating species normally come from the original table of GC-EoS parameters.

The multiphase modeling of CO_2 + hydrocarbons has been a challenge for several models, even when no special constraints were set about depicting the correct transformation between the types of phase behavior shown by the alkane homologous series. Evidence of this fact is that some authors have modeled CO_2 as a self-associating entity, yet it is a nonpolar compound.[4,5] In this work, carbon dioxide is modeled as a nonassociating compound; thus, the new parameters obtained here intend to improve those given in the original GC-EoS[35] and later parametrizations of the model.[36,37] Since methane and ethane are modeled molecularly, as all first compounds of a series, their binary interaction parameters with CO_2 remain the same as the original.

2.1. GCA-EoS Model. There are three contributions to the residual Helmholtz energy (A^R) in the GCA-EoS model:[18] free volume (A^{fv}), attractive (A^{att}), and association (A^{assoc}).

$$A^R = A^{fv} + A^{att} + A^{assoc} \tag{1}$$

The free volume contribution is represented by the extended Carnahan−Starling[38] equation for mixtures of hard spheres developed by Mansoori and Leland[39]

$$\frac{A^{fv}}{RT} = 3\frac{\lambda_1\lambda_2}{\lambda_3}(Y-1) + \frac{\lambda_2^3}{\lambda_3^2}(Y^2 - Y - \ln Y) + n\ln Y \tag{2}$$

with

$$Y = \left(1 - \frac{\pi\lambda_3}{6V}\right)^{-1} \tag{3}$$

$$\lambda_k = \sum_{i=1}^{NC} n_i d_i^k \quad (k = 1, 2, 3) \tag{4}$$

where n_i is the number of moles of component i, NC stands for the number of components, V represents the total volume, R stands for the universal gas constant, T is temperature, and d_i is the hard-sphere diameter per mole of species i.

The following generalized expression gives the temperature dependence of the hard-sphere diameter

$$d_i = 1.065655 d_{ci}\left[1 - 0.12\exp\left(\frac{-2T_{ci}}{3T}\right)\right] \tag{5}$$

where d_{ci} and T_{ci} are, respectively, the critical hard-sphere diameter and critical temperature of component i.

The attraction contribution to the residual Helmholtz energy, A^{att}, accounts for dispersive forces between functional groups. It is a van der Waals expression combined with a density-dependent local-composition mixing rule based on a group contribution version of the NRTL model.[40] The van der Waals expression for the attractive Helmholtz energy is equal to $-a{\cdot}n{\cdot}\rho$, with a being the energy parameter, n the number of moles, and ρ the mole density. For a pure component, a is computed as follows

$$a = \frac{z}{2}q^2 g \tag{6}$$

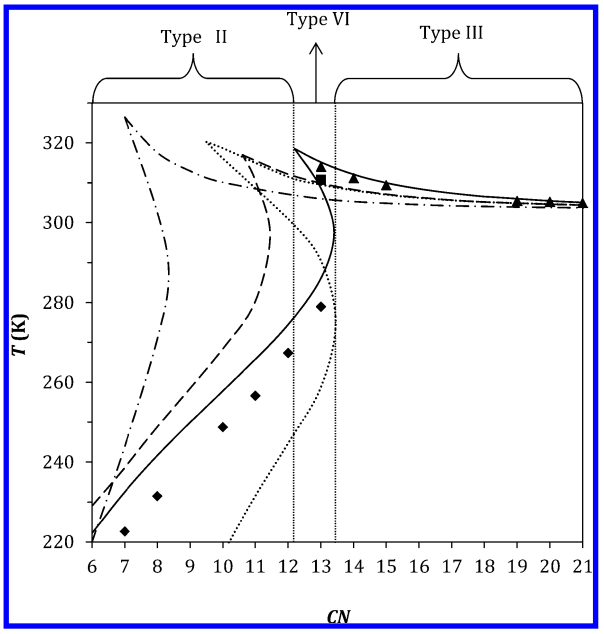

Figure 2. Transformation between types of fluid phase behavior in binary CO_2 + n-alkane systems. Symbols: experimental data[91,105] of UCEP (♦, ▲) and LCEP (■) . Lines: GCA-EoS predictions with previous and current set of parameters: (-·-·) Skjold-Jørgensen,[35] (···) Espinosa et al.,[36] (----) Cismondi et al.,[37] and (—) this work.

where g is the characteristic attractive energy per segment and q is the number of surface segments as defined in the UNIFAC method.[41] The interactions are assumed to take place through the surface, and the coordination number (z) is set equal to 10 as usual.[41] In GCA-EoS the extension to mixtures is carried out using the NRTL model but using local surface fractions like in UNIQUAC[42] rather than local mole fractions

$$\frac{A^{att}}{RT} = -\frac{\frac{z}{2}\tilde{q}^2 g_{mix}}{RTV} \tag{7}$$

where $\tilde{q}$ is the total number of surface segments and g_{mix} is the mixture characteristic attraction energy per total segments and are calculated as follows

$$g_{mix} = \sum_{i=1}^{NG}\theta_i \sum_{j=1}^{NG}\frac{\theta_j\tau_{ij}g_{ij}}{\sum_{k=1}^{NG}\theta_k\tau_{ik}} \tag{8}$$

and

$$\tilde{q} = \sum_{i=1}^{NC}\sum_{j=1}^{NG} n_i\nu_{ij}q_j \tag{9}$$

where ν_{ij} is the number of groups of type j in molecule i, q_j stands for the number of surface segments assigned to group j, θ_j represents the surface fraction of group j

$$\theta_j = \frac{1}{\tilde{q}}\sum_{i=1}^{NC} n_i\nu_{ij}q_j \tag{10}$$

$$\tau_{ij} = \exp\left(\alpha_{ij}\frac{\tilde{q}\Delta g_{ij}}{RTV}\right) \tag{11}$$

$$\Delta g_{ij} = g_{ij} - g_{jj} \tag{12}$$

DOI: 10.1021/acs.iecr.5b03269
Ind. Eng. Chem. Res. 2015, 54, 12415−12427

Table 1. Pure Compound Critical Temperature[44] and Diameter for the Repulsive Contribution of GCA-EoS[a]

compound	T_c (K)	d_c[b] (cm mol$^{-1/3}$)	ARD(P_c) %[c]	ARD(T_c) %[c]	ΔT_r	AARD(P^v) %[d]
carbon dioxide	304.21	3.1287	0.2	0.2	0.71−0.95	1.0
propane	369.83	4.0066	1.3	2.1	0.44−0.95	4.8
isobutane	407.80	4.3511	0.8	2.0	0.45−0.95	3.8
n-butane	425.12	4.3617	0.4	0.8	0.45−0.95	2.8
isopentane	460.40	4.6597	0.2	0.1	0.54−0.95	1.0
n-pentane	469.70	4.6880	0.1	0.7	0.41−0.95	2.6
3-methylpentane	504.60	4.9469	0.9	1.6	0.48−0.95	2.9
n-hexane	507.60	4.9907	0.2	0.2	0.48−0.95	3.4
n-heptane	540.20	5.2726	0.4	0.4	0.50−0.95	3.0
isooctane	543.80	5.4126	0.4	0.4	0.49−0.95	4.6
2,5-dimethylhexane	550.00	5.5232	0.8	3.4	0.50−0.95	3.2
n-octane	568.70	5.5371	0.4	0.5	0.51−0.95	3.0
n-nonane	594.60	5.7868	0.6	1.0	0.52−0.95	2.7
2-methylnonane	610.00	6.0174	0.8	2.7	0.53−0.95	3.7
3-methylnonane	613.00	6.0096	1.1	4.0	0.53−0.95	2.6
4-methylnonane	610.00	6.0281	1.1	5.3	0.52−0.95	2.8
n-decane	617.70	6.0239	0.7	1.2	0.53−0.95	3.4
n-undecane	639.00	6.2497	0.8	1.1	0.54−0.95	3.0
n-dodecane	658.00	6.4659	0.8	1.5	0.55−0.95	2.7
n-tridecane	675.00	6.6739	0.8	0.4	0.56−0.95	2.6
n-tetradecane	693.00	6.8724	1.0	0.1	0.56−0.95	2.8
n-pentadecane	708.00	7.0648	1.0	0.3	0.57−0.95	2.5
n-hexadecane	723.00	7.2506	1.2	0.6	0.58−0.95	2.8
n-octadecane	747.00	7.6079	1.1	1.9	0.60−0.95	3.0
n-nonadecane	758.00	7.7854	1.1	2.6	0.60−0.95	3.1
n-eicosane	768.00	7.9457	0.9	2.8	0.61−0.95	2.5
n-heneicosane	778.00	8.1071	0.9	3.2	0.62−0.95	3.9
n-docosane	787.00	8.2656	0.8	3.1	0.62−0.95	5.5
n-tetracosane	804.00	8.5717	0.7	3.9	0.63−0.95	3.3
n-octacosane	832.00	9.1479	0.4	5.3	0.65−0.95	4.8
n-dotriacontane	855.00	9.6921	0.1	7.1	0.66−0.95	5.9
n-hexatriacontane	874.00	10.183	0.3	9.1	0.68−0.95	9.0

[a]GCA-EoS deviations in the prediction of critical properties and vapor pressure within the reduced temperature range, ΔT_r. [b]Critical diameter fitted to a pure compound saturation point. [c]ARD: Absolute relative deviation with respect to experimental data[44] = $100 \times |(z_{exp} - z_{calc})/z_{exp}|$.[44] [d]AARD: Average absolute relative deviation with respect to experimental data[44] = $(100/N) \sum_i^N |(z_{exp\ i} - z_{calc\ i})/z_{exp\ i}|$.

g_{ij} is the attractive energy between groups i and j and α_{ij} is the nonrandomness parameter. It is worth highlighting that in the absence of nonrandomness ($\alpha_{ij} = 0$), eq 8 gives the classical quadratic mixing rule.

The attractive energy, g_{ij}, is calculated from the energy between like-group segments through the following combination rule

$$g_{ij} = k_{ij}\sqrt{g_{ii}g_{ji}} \quad (k_{ij} = k_{ji}) \tag{14}$$

with the following temperature dependence for the energy and interaction parameters

$$g_{ii} = g_{ii}^*\left[1 + g_{ii}'\left(\frac{T}{T_i^*} - 1\right) + g_{ii}''\ln\left(\frac{T}{T_i^*}\right)\right] \tag{15}$$

and

$$k_{ij} = k_{ij}^*\left[1 + k_{ij}'\ln\left(\frac{2T}{T_i^* + T_j^*}\right)\right] \tag{16}$$

where g_{ii}^* is the attraction energy and k_{ij}^* the interaction parameter at the reference temperature T_i^* and $(T_i^* + T_j^*)/2$, respectively.

Finally, the association term,[18] A^{assoc}, is a group contribution version of the SAFT equation of Chapman et al.[43]

$$\frac{A^{assoc}}{RT} = \sum_{i=1}^{NGA} n_i^*\left[\left(\sum_{k=1}^{M_i}\ln X_{ki} - \frac{X_{ki}}{2}\right) + \frac{M_i}{2}\right] \tag{17}$$

In this equation NGA represents the number of associating functional groups, n_i^* the total number of moles of associating group i, X_{ki} the fraction of group i nonbonded through site k, and M_i the number of associating sites in group i. The total number of moles of associating group i is calculated from the number ν_{mi}^* of associating groups i present in molecule m and the total amount of moles of specie m (n_m)

$$n_i^* = \sum_{m=1}^{NC}\nu_{mi}^* n_m \tag{18}$$

The fraction of groups i nonbonded through site k is determined by the expression

$$X_{ki} = \left(1 + \sum_{j=1}^{NGA}\sum_{l=1}^{M_j}\frac{n_j^* X_{lj}\Delta_{ki,lj}}{V}\right)^{-1} \tag{19}$$

DOI: 10.1021/acs.iecr.5b03269
Ind. Eng. Chem. Res. 2015, 54, 12415−12427

where the summation includes all *NGA* associating groups and M_j sites. X_{ki} depends on the association strength, $\Delta_{ki,lj}$

$$\Delta_{ki.lj} = \kappa_{ki.lj}\left[\exp\left(\frac{\varepsilon_{ki,lj}}{RT}\right) - 1\right] \tag{20}$$

The association strength between site k of group i and site l of group j depends on the temperature T and on the association parameters $\kappa_{ki,jl}$ and $\varepsilon_{ki,jl}$, which represent the volume and energy of association, respectively.

The parametrization procedure was performed through optimization of the following objective function

$$\text{O. F.} = \sum_{i=j}^{\text{NE}_q} e_{\text{eq}i}^2 \tag{21}$$

where NE_q is the number of experimental points in the correlation database and $e_{\text{eq}i}$ are the relative deviations between experimental and calculated data as follows

$$e_{\text{eq}i}^2 = \text{IFL}_i wp_i^2 (P_{\text{exp}\,i} - P_{\text{calcd}\,i})^2 + (1 - \text{IFL}_i) wx_i^2 \times (x_{\text{exp}\,i} - x_{\text{calcd}\,i})^2 + wy_i^2 (y_{\text{exp}\,i} - y_{\text{calcd}\,i})^2 \tag{22}$$

where P is the pressure, x and y are the molar fraction in the liquid and vapor phase, and wp_i, wx_i, and wy_i are the weighting factors of P, x, and y. IFL is an auxiliary variable which sets the type of flash calculation: 0 for a *TP* flash and 1 for bubble point calculations. In this work, all VLE data was simulated through bubble point calculations while the LLE data were via *TP* flashes. Furthermore, the weighting factor of each experimental data was set equal to the inverse of its value. Nonetheless, in the case of the two data points closest to each critical point, their weighting factors were also increased by a factor of 10. This methodology allowed achieving a better critical locus representation of the correlated systems. The objective function (eq 21) was minimized employing the Levenberg–Marquardt algorithm of finite difference coded in Fortran77.

GCA-EoS correlation is laborious due to the density-dependent mixing rule and the group contribution approach (different compounds share the same binary interaction parameters). In this work the parametrization was performed fitting binary VLE data of *n*-butane and *n*-decane and the VLLE data of CO_2 + *n*-tridecane. The latter induces the model to depict a Type IV phase behavior in the correct transition binary system. The new binary interaction parameters were determined based on the pure group parameters already set in previous works.[21,35] The initial values of the binary parameters were set so that the mixing rules of the model were reduced to the classical van der Waals one fluid (i.e., $k_{ij}^* = 1$, $k_{ij}' = \alpha_{ij} = \alpha_{ji} = 0$). Moreover, interaction parameters between CO_2 and paraffinic groups (CH_3 and CH_2) were assumed equal until the final optimization. In a first step, only k_{ij}^* was allowed to change, next its temperatures dependence k_{ij}', and last the nonrandomness parameters (α_{ij} and α_{ji}). Any parameter that did not improve substantially the fitting was set back to its initial value. Finally, the interaction parameters between CO_2 and the paraffinic groups were allowed to accomplish different values. All those parameters that during the parametrization were left in its initial value were challenged to improve the final correlation, but again, if the result did not improved substantially, the parameter under evaluation was left in its original value.

Table 2. GCA-EoS Pure Group Parameters for the Attractive Contribution

group i	q_i	T_i^* (K)	g_i^* (atm cm^6 mol^{-2})	g_i'	g_i''	ref
CH_3	0.848	600.0	316 910	−0.9274	0	35
CH_2	0.540	600.0	356 080	−0.8755	0	35
$CHCH_3$	1.076	600.0	303 749	−0.8760	0	21
(B)CH_3	0.848	600.0	282 715	−0.6393	0	21
(B)CH_2	0.540	600.0	294 523	−0.8233	0	21
CO_2	1.261	304.2	531 890	−0.5780	0	35

Table 3. Binary Energy Interaction Parameters Fitted in This Work

groups					
i	j	k_{ij}^*	k_{ij}'	α_{ij}	α_{ji}
CO_2	CH_3/(B)CH_3	0.9185	0.0469	−26.0	4.0
	CH_2/(B)CH_2/$CHCH_3$	0.9100	0.0469	−21.0	0

3. RESULTS AND DISCUSSION

3.1. Phase Behavior Modeling of Carbon Dioxide + *n*-Alkane Mixtures. As already introduced, in order to develop a robust model to predict multiphase behavior, it is also important to challenge the model to follow up the transformation between types of phase behavior as the alkyl chain length increases. As we will show next, the three previous parametrization of CO_2/alkyl-group binary interaction portray incorrectly this transformation (see Figure 2). Of course, a wrong prediction of the type of binary phase behavior will lead to false heterogeneous regions for particular mixtures and, consequently, also for multicomponent systems. It is important to bear in mind that the fitted parameters of a group contribution model will affect not only the behavior of CO_2 + alkanes mixtures but also other alkyl derivative compounds. In fact, we faced the need to review CO_2/alkyl group binary interaction of GCA-EoS when we found it infeasible to attain accurate

Table 4. GCA-EoS Phase Behavior Correlation of CO_2 + *n*-Alkanes Binary Systems[a]

alkane	T (K)	P (bar)	AARD(P) %	AARD(y_1) %	N	ref
vapor–liquid equilibria						
n-butane	311	4–75	1.5	1.0	21	45
n-decane	278, 444	3–188	5.5	0.15	25	46

			AAD(AARD %)			
alkane	T (K)	P (bar)	CO_2 in HC	HC in CO_2	N	ref
vapor–liquid–liquid equilibria						
n-tridecane	255–314	21–87	0.014 (1.8)	0.011 (33)	29	47, 48

[a]AAD and AARD%: average absolute and relative deviations in pressure (P) and composition (x/y), respectively.

DOI: 10.1021/acs.iecr.5b03269
Ind. Eng. Chem. Res. 2015, 54, 12415–12427

Table 5. GCA-EoS Phase Behavior Prediction of CO_2 + *n*-Alkanes Binary Systems[a]

alkane	T (K)	P (bar)	AARD(P) %	AARD(y_1) %	N	ref
			vapor−liquid equilibria			
n-propane	240−361	3.0−65	4.1	3.1	173	49−52
n-butane	227−418	0.35−82	2.2	2.5	519	45−59
n-pentane	277−463	2.0−96	2.6	2.6	110	60−62
n-hexane	303−393	8.0−116	1.7	0.63	65	63,64
	273−303	10−60	1.1		24	65
n-heptane	310−477	2.0−133	8.6	0.86	62	66
	310−413	23−134	8.6		117	67
n-octane	313−372	15−137	2.3	0.23	48	68,69
n-nonane	315−418	20−167	7.7	0.43	44	70,71
n-decane	310−584	7.0−186	4.5	0.66	174	46,68,71−74
	344	9.0−127	3.1		31	75,76
n-undecane	315−418	20−200	4.0	0.22	42	70
n-dodecane	318	10−90	3.5	0.20	10	77
	313−343	1.0−143	4.6		56	78,79
n-tetradecane	290, 311	9.0−40	15		18	80
n-pentadecane	293−303	6.0−70	7.0	0.19	22	81,82
n-hexadecane	296, 297	4.0−16	9.5		4	83
			AAD(AARD %) of x_i in j			
alkane	T (K)	P (bar)	CO_2 in HC	HC in CO_2	N	ref
			liquid−liquid equilibria			
n-pentadecane	293−303	56−141	0.021 (2.6)	0.020 (96)	19	81,82
			liquid−supercritical fluid equilibria			
n-tetradecane	331, 344	14−164	0.022 (5.6)		24	84
n-tetradecane	344	71−163		6.9×10^{-3} (44)	22	84
n-pentadecane	313−353	5.1−175	0.023 (6.2)	6.0×10^{-3} (228)	46	81
	313	16−64	0.028 (7.3)		8	85
n-hexadecane	314−664	20−257	0.024 (4.7)	8.1×10^{-3} (33)	64	72,86−89
	313, 333	17−145	0.026 (5.1)		17	78,84
	313, 323	98−153		0.019 (75)	7	78
n-octadecane	310−353	100−200	0.068 (9.8)	7.7×10^{-3} (129)	32	90
n-nonadecane	313, 333	3.0−87.0	0.024 (7.1)		47	91,92
n-eicosane	310−473	5.0−344	0.021 (5.8)		135	78,83,93−96
	315−348	100−320		7.7×10^{-3} (113)	14	98
n-eneicosane	318−338	9.0−78	0.018 (5.0)		26	91
n-docosane	323−473	10−373	0.020 (4.1)		75	93,97
n-tetracosane	373−573	10−300	0.013 (7.8)	4.3×10^{-4} (21)	15	98
	330−473	94−389	0.016 (2.2)		37	78,93
	330−357	190−283		7.9×10^{-3} (172)	11	78
n-octacosane	338−473	8.0−408	0.015 (4.0)		60	78,93,94,99
	308−366	119−327		4.1×10^{-3} (156)	77	78
	573	10−50.0	0.019 (10)	1.5×10^{-4} (5.7)	5	99
n-dotriacontane	373−573	10−400	0.023 (7.1)	1.1×10^{-3} (66)	21	86,98
	348, 373, 398	9.0−72.0	0.018 (5.8)		37	97
n-hexatriacontane	344−423	5.2−298	0.013 (4.4)		33	78,94
	344−366	223−292		1.4×10^{-3} (146)	17	78
n-tetratetracontane	373−423	6.0−71	0.048 (19)		14	94
			vapor−liquid−liquid equilibria			
n-octane	216−231	5−9	0.12 (19)		18	100
	215−226	5−9		0.019 (35)	12	100
n-decane	235−248	11−16	0.078 (11)	0.024 (36)	9	101
n-dodecane	254−267	20−29	0.028 (3.4)	0.011 (11)	8	47
n-tetradecane	269−303	30−83	0.012 (1.5)	0.010 (33)	23	47
n-pentadecane	207−308	32−80	0.035 (4.7)	0.012 (69)	16	47,102
n-hexadecane	283−306	44−78	0.040 (5.5)	9×10^{-3} (91)	6	102
n-nonadecane	293−304	58−74	0.052 (7.3)	5.1×10^{-3} (193)	17	91
n-eicosane	300−305	68−75	0.048 (6.7)	2.2×10^{-3} (296)	37	91,95
n-eneicosane	302−304	71−75	0.050 (7.0)	1.1×10^{-3} (205)	10	91

[a]AAD and AARD %: average absolute and relative deviations, in pressure (P) and composition (x/y), respectively.

DOI: 10.1021/acs.iecr.5b03269
Ind. Eng. Chem. Res. 2015, 54, 12415−12427

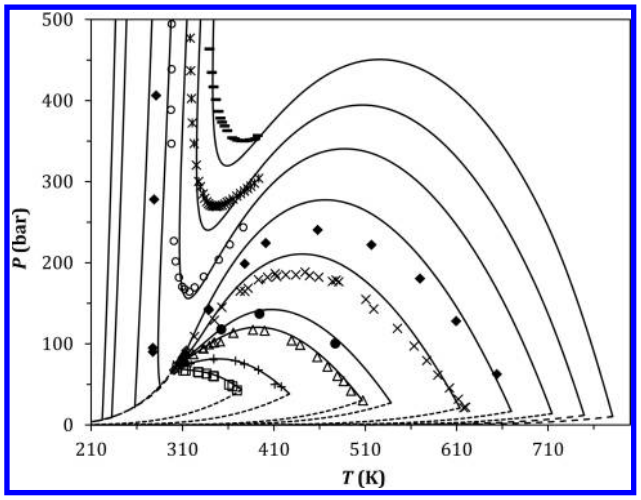

Figure 3. *PT* projection of the phase equilibria of selected CO_2 + *n*-alkane binary systems: (□) propane, (+) *n*-butane, (△) *n*-hexane, (●) *n*-heptane, (×) *n*-decane, (♦) *n*-tridecane, (○) *n*-hexadecane, (*) *n*-nonadecane, and (■) *n*-docosane. Symbols: experimental data.[45,47,48,53,54,61,66,90,106−111] Solid lines: GCA-EoS predictions of critical lines. Dashed lines: GCA-EoS prediction of pure compound vapor pressure curves.

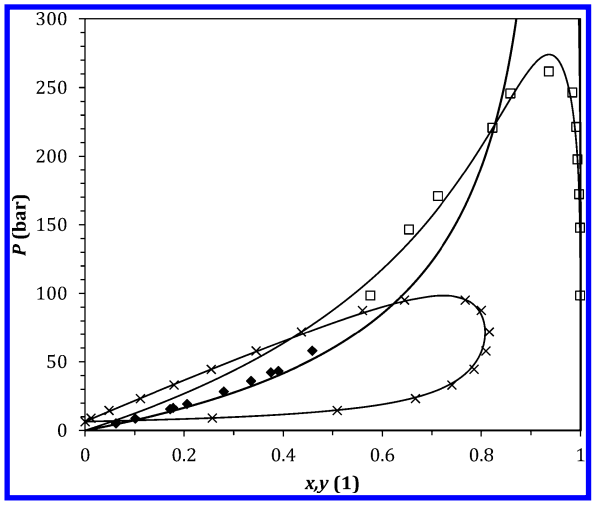

Figure 4. Vapor−liquid equilibria of CO_2 (1) + *n*-alkane (2) binary systems: (×) *n*-pentane at 377 K, (□) *n*-octadecane, and (◆) *n*-hexatriacontane at 373 K. Symbols: experimental data.[60,90,94] Solid lines: GCA-EoS predictions.

multiphase prediction of CO_2 with *n*-alcohols homologous series, based on the available interaction parameters.

Before fitting the binary interaction, it is important to check whether the model is able to correctly predict the critical properties of pure paraffins. This is usually the case for molecular models, since the pure compound parameters are set on the basis of fulfilling the critical point and its conditions (null value of the first and second pressure derivative with respect to the volume). However, in a group contribution model, this is not the case as the same two groups (CH_2 and CH_3) have to describe the vapor pressure curve of the whole *n*-alkane homologous family. Moreover, the branched paraffins, also considered in this work, share the $CHCH_3$ and the bulky alkyl groups, $(B)CH_3$ and $(B)CH_2$, when linked to a quaternary carbon. Tables 1 and 2 give the critical temperature and diameter for the free volume contribution and the pure surface

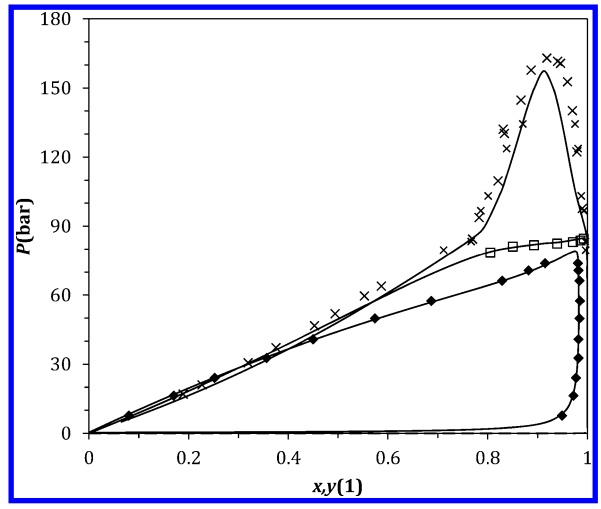

Figure 5. Vapor−liquid equilibria of CO_2 (1) + *n*-alkane (2) binary systems at 313 K: (◆) *n*-hexane, (□) *n*-dodecane, and (×) *n*-hexadecane. Symbols: experimental data.[63,64,78,85,89] Solid lines: GCA-EoS predictions.

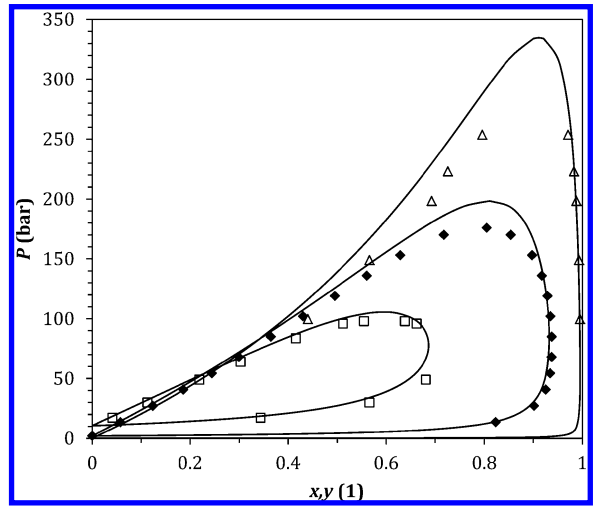

Figure 6. Vapor−liquid equilibria of CO_2 (1) + *n*-alkane (2) binary systems at 477 K: (□) *n*-heptane, (◆) *n*-decane, and (△) *n*-hexadecane. Symbols: experimental data.[46,66,88] Solid lines: GCA-EoS predictions.

energy parameters for the attractive term, respectively. Moreover, Table 1 also reports GCA-EoS accuracy to predict the critical point and the vapor pressure curve of all compounds considered in this work. In summary, GCA-EoS performs very well for the 32 compounds under study.

Table 3 reports the only binary interaction parameters fitted for the attractive term in this work. It is worth mentioning that the 31 binary systems are modeled based on no more than these 8 binary interaction parameters. Tables 4 and 5 show the GCA-EoS accuracy to correlate and predict binary equilibrium data of CO_2 + *n*-alkanes, respectively. The tables also report the temperature and pressure range of the experimental data, number of data points (*N*), and source of the experimental data for each binary system. These results bring to light the main advantage of applying a group contribution approach. Common molecular models require at least 31 binary interaction parameters to describe the systems tested here. However, it is unlikely that a model can predict the results shown here for a wide temperature range with temperature-independent interaction

DOI: 10.1021/acs.iecr.5b03269
Ind. Eng. Chem. Res. 2015, 54, 12415−12427

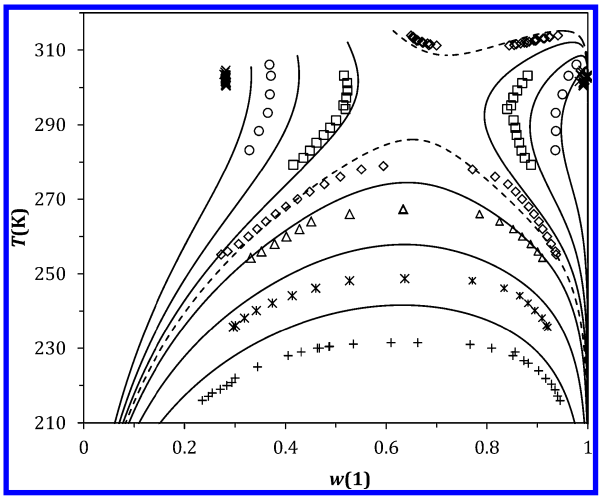

Figure 7. Vapor−liquid−liquid equilibria of CO_2 (1) + *n*-alkane binary systems: (+) *n*-octane, (*) *n*-decane, (△) *n*-dodecane, (◊) *n*-tridecane, (□) *n*-tetradecane, (○) *n*-hexadecane, and (×) *n*-eicosane. Symbols: experimental data.[47,100−102] Dashed and solid lines: GCA-EoS correlation and prediction, respectively.

parameters, meaning that at least 62 parameters would be needed. In conclusion, the GCA-EoS requires 7 times less binary interaction parameters.

Figure 2 shows the experimental upper and lower critical end points for the CO_2 + *n*-alkane binary systems as the alkyl chain increases. These data allow inferring the type of phase behavior for each binary and, consequently, its transformation within the homologous family, namely, binary behavior changing from Type II (lower than C_{12}) to III (higher than C_{14}), going through Type IV at *n*-tridecane. Figure 2 also depicts GCA-EoS predictions using the previous sets of parameters and the new set proposed in this work. The phase behavior of carbon dioxide + *n*-alkanes binary systems was originally modeled with the GC-EoS by Skjold-Jørgensen,[34] who considered only VLE data of mixtures containing hydrocarbons up to *n*-decane. Even though this original parametrization performs well within the correlated systems, it presents serious failures when dealing with heavier hydrocarbons. To overcome this, Espinosa et al.[36] proposed a different set of binary interaction parameters for specifically modeling high molecular weight fatty compounds. The parametrization improved the description of heavy hydrocarbons (up to *n*-tetradecane) while keeping precise VLE predictions for light hydrocarbons (from propane to *n*-heptane). The work of Espinosa provided accurate mutual solubility of CO_2 and fatty compounds up to 400 bar, but it was unable to predict binary critical points. Later, Cismondi et al.[37] did an ad hoc parametrization of the binary interaction between CO_2 and the alkyl groups, correlating also critical points[103,104] of fatty compounds with CO_2. By this way the authors solved the previous overestimation of immiscible regions. As evident from Figure 2, the parametrization provided by Skjold-Jørgensen predicts the transition Type IV between *n*-heptane and *n*-octane. Parameters provided by Espinosa et al.[36] predict a Type IV behavior from *n*-decane up to *n*-tridecane. In contrast, those of Cismondi et al.[37] predict the transition in *n*-undecane. Consistent with the parametrization strategy of this work, the new set of parameters correctly reproduces the transition at *n*-tridecane.

Figure 3 shows the prediction of the critical loci of selected binary systems. Overall, a very good description is obtained for all the series. The reader should keep in mind that a good description of the *PT* projection of the whole *n*-alkane family means that the model will perform well in multiphase behavior with a single set of parameters.

Figures 4−6 depict the model accuracy to predict VLE and VLLE of selected binary systems using the new set of parameters. It is interesting to see how well the model predicts the change in phase behavior with the length of the alkyl chain. Figure 7 shows that GCA-EoS also adequately predicts changes from miscible to partially miscible or completely immiscible behavior.

Since we report a set of parameters covering equilibrium data under a wide range of temperature and pressure, it is expected that the model correctly predicts excess property data of CO_2+alkanes binary systems. As examples, Figures 8 and 9

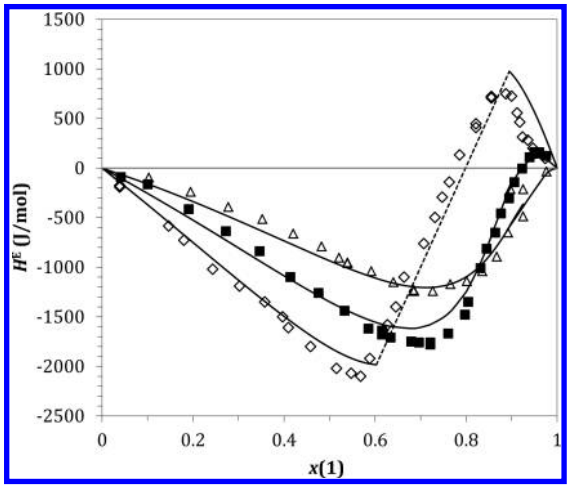

Figure 8. Excess enthalpy of CO_2 (1) + *n*-pentane (2) binary system at 348 K and (◊) 75 bar, (■) 105 bar, and (△) 125 bar. Symbols: experimental data.[112] Solid lines: GCA-EoS predictions. Dotted line: two-phase mixture.

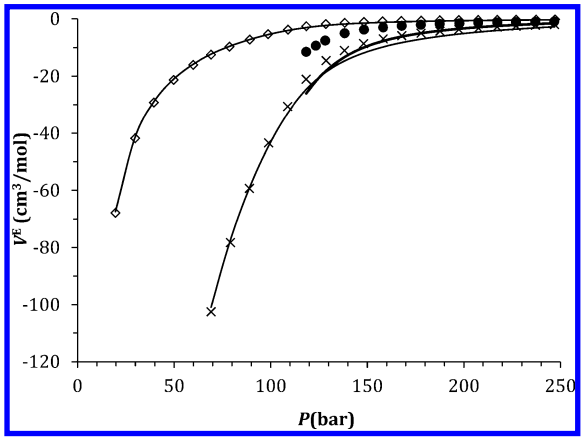

Figure 9. Excess volume of CO_2 (1) + *n*-decane (2) binary system at 333 K and different carbon dioxide molar compositions: (◊) 0.0551, (×) 0.4536, and (●) 0.9663.[113] Solid lines: GCA-EoS predictions.

show the model predictions of excess enthalpy of CO_2 + *n*-pentane and excess volume of CO_2 + *n*-decane, data available in the open literature,[112,113] respectively.

3.2. Phase Behavior Prediction of Carbon Dioxide + Branched Alkanes. Extension of the GCA-EoS to branched

DOI: 10.1021/acs.iecr.5b03269
Ind. Eng. Chem. Res. 2015, 54, 12415−12427

Table 6. GCA-EoS Phase Behavior Prediction of CO_2 (1) + Branched Alkanes (2) Binary Systems[a]

alkane	T (K)	P (bar)	N	AARD(P)%	AARD(y_1)%	ref
isobutane	250−398	0.64−67	122	3.1	2.4	53,56,114
isopentane	277−453	0.42−83	70	2.3	4.6	61,115
3-methylpentane	293−383	28−102	40	8.6		67
isooctane	270−393	12−106	184	5.0		67,116,117
	323−348	21−28	6		6.8	118
2.5-dimethylhexane	278−413	25−116	101	9.3		67
2-methylnonane	308−349	57−131	42	2.3		119
3-methylnonane	308−348	54−134	37	1.7		119
4-methylnonane	308−348	59−124	49	1.4		119

[a]AARD %: average absolute relative deviations in pressure (P) and composition (y).

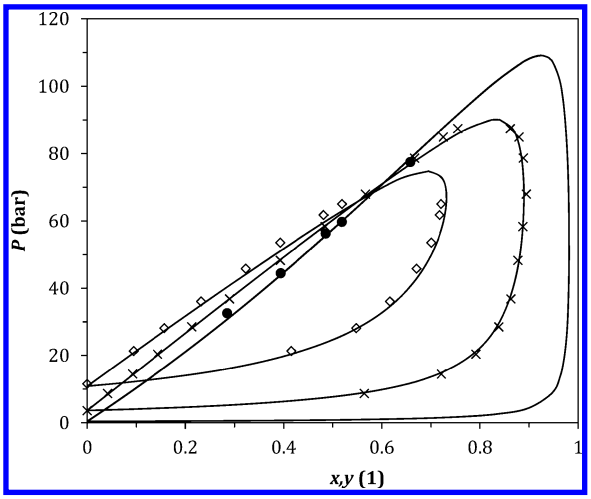

Figure 10. Vapor−liquid equilibria of CO_2 (1) + branched alkane (2) binary systems at 344 K: (◊) isobutane, (×) isopentane, and (●) isooctane. Symbols: experimental data.[67,114,115] Solid lines: GCA-EoS predictions.

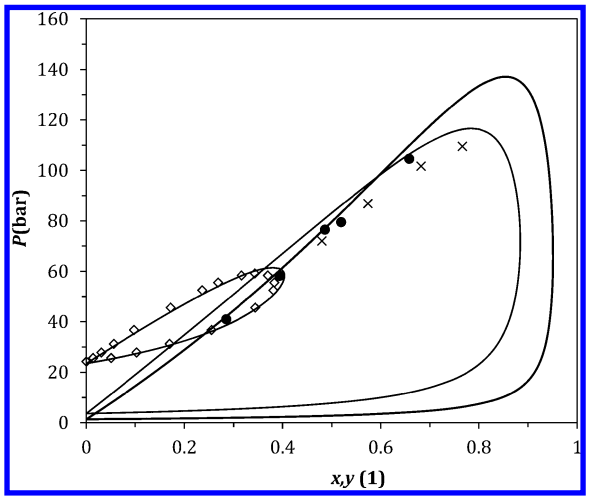

Figure 11. Vapor−liquid equilibria of CO_2 (1) + branched alkanes (2) binary systems at 383 K: (◊) isobutane, (×) 3-metylpentane, and (●) isooctane Symbols: experimental data.[53,67] Solid lines: GCA-EoS predictions.

alkanes was revised by Soria et al.[21] As mentioned before, in order to build a branched alkane molecule, the bulky groups are needed: (B)CH_3 and (B)CH_2 for alkyl groups bonded to quaternary carbon atoms and $CHCH_3$ for ternary carbon atoms. These three groups have different surface energy than that of CH_2 and CH_3 groups (see Table 2). However, their binary energy interaction with CO_2 was set the same, as shown in Table 3. Table 6 shows the GCA-EoS accuracy to predict VLE data. The table summarizes the temperature and pressure range of the experimental data, GCA-EoS average deviations in bubble point calculation, the number of experimental data points (N), and the source of experimental data. Figures 10 and 11 depict results for selected branched alkanes with CO_2. Using the interaction parameters derived from linear alkanes, the agreement in most cases is highly accurate, considering that it is fully predicted data.

4. CONCLUSIONS

The GCA-EoS has been reviewed to model mixtures of carbon dioxide with the homologous family of *n*-alkanes. The model was tested against an experimental database covering C_3−C_{36} alkanes, temperatures from 210 to 660 K, and pressures up to 400 bar. The wide range of conditions and the parametrization strategy are keys to developing a robust thermodynamic tool for predicting multiphase behavior. Previous parametrizations of the GCA-EoS are not able to follow the transformation between types of fluid phase behavior in CO_2 + *n*-alkane binary mixtures. In this work, special attention was given to this transformation in order to develop a multiphase predictive model. If a model does not follow the type of phase behavior, it either overestimates the immiscible regions or does not predict the liquid phase split for particular systems. The new set of binary interaction parameters between CO_2 and the alkyl groups correctly represents the transformation between types of phase behavior. Moreover, we show that the revised set of binary parameters also depicts accurate predictions for branched alkanes.

The density-dependent mixing rules of this model are laborious to fit. However, they give enough flexibility to reproduce the global phase diagrams without affecting the quality of bubble and dew curve calculations. It is worth highlighting that the same set of parameters accomplishes accurate results both in subcritical and in critical regions for the whole alkane family. The liquid−liquid calculations are less accurate in some cases; nevertheless, the VLLE is always qualitatively modeled. Prediction of multiphase behavior with a single set of parameters is a key point when developing a model for new processes and product design.

AUTHOR INFORMATION

Corresponding Author

*E-mail: spereda@plapiqui.edu.ar. Phone: + 54 291 4861700. Fax: +54 291 4861600.

DOI: 10.1021/acs.iecr.5b03269
Ind. Eng. Chem. Res. 2015, 54, 12415−12427

Notes

The authors declare no competing financial interest.

■ ACKNOWLEDGMENTS

The authors acknowledge the financial support granted by the Consejo Nacional de Investigaciones Científicas y Técnicas (CONICET), the Ministerio de Ciencia, Tecnología e Innovación Productiva (MinCyT), and the Universidad Nacional del Sur (UNS).

■ LIST OF SYMBOLS

A	Helmholtz free energy
AAD(Z)	average absolute deviation in variable Z: $(1/N)\sum_i^N \lvert Z_{\mathrm{exp}\,i} - Z_{\mathrm{calc}\,i}\rvert$
ARD(Z)%	absolute relative deviation in variable Z: $100 \lvert (Z_{\mathrm{exp}\,i} - Z_{\mathrm{calcd}\,i}/Z_{\mathrm{exp}\,i})\rvert$
AARD(Z)%	average absolute relative deviation in variable Z: $(100/N)\sum_i^N \lvert (Z_{\mathrm{exp}\,i} - Z_{\mathrm{calcd}\,i}/Z_{\mathrm{exp}\,i})\rvert$
CN	carbon number
CP	critical point
d_i	effective hard-sphere diameter of component i
d_{ci}	effective hard-sphere diameter of component i evaluated at T_c
g_{ij}	group energy interaction per surface segment between groups i and j
HC	hydrocarbon
IFL	auxiliary variable for objective function calculation in eq 22
k_{ij}	binary interaction parameter between groups i and j
LLE	liquid−liquid equilibria
N	number of experimental points of each data set
NC	number of components in the mixture
NG	number of attractive groups in the mixture
NGA	number of associating groups in the mixture
M_i	total number of associating sites in group i
P	pressure
q_j	number of surface segments of group j
R	Universal gas constant
T	temperature
T_{ci}	critical temperature of component i
UCEP	upper critical end point
UCST	upper critical solution temperature
V	total volume of the mixture
VLE	vapor−liquid equilibria
w_i	mass composition of component i
wp, wx, wy	weight factors for pressure, liquid, and vapor composition, respectively, in eq 22
X_{ki}	fraction of nonbonded associating sites of type k in group i
x_i	molar composition in liquid phase of component i
y_i	molar composition in vapor phase of component i
Z	dummy variable
z	coordination number

Greek Symbols

α_{ij}	nonrandomness parameter between groups i and j
ΔZ%	ARD% in variable Z
$\varepsilon_{ki,lj}$	energy of association between site k of group i and site l of group j
$\kappa_{ki,lj}$	volume of association between site k of group i and site l of group j
ν_{ij}	number of groups j in compound i
ν_{ij}^{*}	number of associating groups j in compound i

■ REFERENCES

(1) Konynenburg, P. H. V.; Scott, R. L. Critical Lines and Phase Equilibria in Binary Van Der Waals Mixtures. *Philos. Trans. R. Soc., A* **1980**, *298* (1442), 495.

(2) Brignole, E. A.; Pereda, S. Phase Equilibrium Engineering Principles in Reactive Systems. In *Phase Equilibrium Engineering*; Brignole, E. A., Pereda, S., Eds.; Elsevier B.V.: Amsterdam, 2013; Vol. 3, pp 263−298.

(3) Coutinho, J. A. P.; Kontogeorgis, G. M.; Stenby, E. H. Binary Interaction Parameters for Nonpolar Systems with Cubic Equations of State: A Theoretical Approach 1. CO2/hydrocarbons Using SRK Equation of State. *Fluid Phase Equilib.* **1994**, *102*, 31.

(4) Oliveira, M. B.; Queimada, A. J.; Kontogeorgis, G. M.; Coutinho, J. A. P. Evaluation of the CO2 Behavior in Binary Mixtures with Alkanes, Alcohols, Acids and Esters Using the Cubic-Plus-Association Equation of State. *J. Supercrit. Fluids* **2011**, *55* (3), 876.

(5) Tsivintzelis, I.; Kontogeorgis, G. M.; Michelsen, M. L.; Stenby, E. H. Modeling Phase Equilibria for Acid Gas Mixtures Using the CPA Equation of State. Part II: Binary Mixtures with CO2. *Fluid Phase Equilib.* **2011**, *306* (1), 38.

(6) Hsieh, C.-M.; Windmann, T.; Vrabec, J. Vapor−Liquid Equilibria of CO2 + C1−C5 Alcohols from the Experiment and the COSMO-SAC Model. *J. Chem. Eng. Data* **2013**, *58* (12), 3420.

(7) Grenner, A.; Kontogeorgis, G. M.; von Solms, N.; Michelsen, M. L. Modeling Phase Equilibria of Alkanols with the Simplified PC-SAFT Equation of State and Generalized Pure Compound Parameters. *Fluid Phase Equilib.* **2007**, *258* (1), 83.

(8) Horstmann, S.; Fischer, K.; Gmehling, J.; Kolář, P. Experimental Determination of the Critical Line for (carbon Dioxide + Ethane) and Calculation of Various Thermodynamic Properties for (carbon Dioxide + n-Alkane) Using the PSRK Model. *J. Chem. Thermodyn.* **2000**, *32* (4), 451.

(9) Vitu, S.; Privat, R.; Jaubert, J.-N.; Mutelet, F. Predicting the Phase Equilibria of CO2+hydrocarbon Systems with the PPR78 Model (PR EOS and Kij Calculated through a Group Contribution Method). *J. Supercrit. Fluids* **2008**, *45* (1), 1.

(10) Nguyen-Huynh, D.; Passarello, J.-P.; Tobaly, P.; de Hemptinne, J.-C. Modeling Phase Equilibria of Asymmetric Mixtures Using a Group-Contribution SAFT (GC-SAFT) with a Kij Correlation Method Based on London's Theory. 1. Application to CO2 + N-Alkane, Methane + N-Alkane, and Ethane + N-Alkane Systems Dong. *Ind. Eng. Chem. Res.* **2008**, *47* (22), 8847.

(11) Polishuk, I.; Wisniak, J.; Segura, H. Simultaneous Prediction of the Critical and Sub-Critical Phase Behavior in Mixtures Using Equation of State I. Carbon Dioxide-Alkanols. *Chem. Eng. Sci.* **2001**, *56* (23), 6485.

(12) Polishuk, I.; Wisniak, J.; Segura, H. Simultaneous Prediction of the Critical and Sub-Critical Phase Behavior in Mixtures Using Equations of State II. Carbon Dioxide−heavy N-Alkanes. *Chem. Eng. Sci.* **2003**, *58* (12), 2529.

(13) Polishuk, I.; Wisniak, J.; Segura, H. Estimation of Liquid−Liquid−Vapor Equilibria Using Predictive EOS Models. 1. Carbon Dioxide - N -Alkanes. *J. Phys. Chem. B* **2003**, *107* (8), 1864.

(14) Cismondi, M.; Rodríguez-Reartes, S. B.; Milanesio, J. M.; Zabaloy, M. S. Phase Equilibria of CO2 + N-Alkane Binary Systems in Wide Ranges of Conditions: Development of Predictive Correlations Based on Cubic Mixing Rules. *Ind. Eng. Chem. Res.* **2012**, *51* (17), 6232.

(15) Galindo, A.; Blas, F. J. Theoretical Examination of the Global Fluid Phase Behavior and Critical Phenomena in Carbon Dioxide + N -Alkane Binary Mixtures. *J. Phys. Chem. B* **2002**, *106* (17), 4503.

(16) García, J.; Lugo, L.; Fernández, J. Phase Equilibria, PVT Behavior, and Critical Phenomena in Carbon Dioxide + N-Alkane Mixtures Using the Perturbed-Chain Statistical Associating Fluid Theory Approach. *Ind. Eng. Chem. Res.* **2004**, *43* (26), 8345.

(17) Llovell, F.; Vega, L. F. Global Fluid Phase Equilibria and Critical Phenomena of Selected Mixtures Using the Crossover Soft-SAFT Equation. *J. Phys. Chem. B* **2006**, *110* (3), 1350.

DOI: 10.1021/acs.iecr.5b03269
Ind. Eng. Chem. Res. 2015, 54, 12415−12427

(18) Gros, H. P.; Bottini, S. B.; Brignole, E. A. A Group Contribution Equation of State for Associating Mixtures. *Fluid Phase Equilib.* **1996**, *116* (1−2), 537.
(19) Soria, T. M.; Sánchez, F. A.; Pereda, S.; Bottini, S. B. Modeling Alcohol+water+hydrocarbon Mixtures with the Group Contribution with Association Equation of State GCA-EoS. *Fluid Phase Equilib.* **2010**, *296* (2), 116.
(20) Sánchez, F. A.; Pereda, S.; Brignole, E. A. GCA-EoS: A SAFT Group Contribution model—Extension to Mixtures Containing Aromatic Hydrocarbons and Associating Compounds. *Fluid Phase Equilib.* **2011**, *306* (1), 112.
(21) Soria, T. M.; Andreatta, A. E.; Pereda, S.; Bottini, S. B. Thermodynamic Modeling of Phase Equilibria in Biorefineries. *Fluid Phase Equilib.* **2011**, *302* (1−2), 1.
(22) Soria, T. M.; Sánchez, F. A.; Pereda, S.; Bottini, S. B. Modeling the Phase Behavior of Cyclic Compounds in Mixtures of Water, Alcohols and Hydrocarbons. *Fluid Phase Equilib.* **2014**, *361*, 143.
(23) Sánchez, F. A.; Mohammadi, A. H.; Andreatta, A. E.; Pereda, S.; Brignole, E. A.; Richon, D. Phase Behavior Modeling of Alkyl Amine + Hydrocarbon and Alkyl Amine + Alcohol Systems Using a Group Contribution Associating Equation of State. *Ind. Eng. Chem. Res.* **2009**, *48* (16), 7705.
(24) Sánchez, F. A.; Soria, T. M.; Pereda, S.; Mohammadi, A. H.; Richon, D.; Brignole, E. A. Phase Behavior Modeling of Alkyl - Amine + Water Mixtures and Prediction of Alkane Solubilities in Alkanolamine Aqueous Solutions with Group Contribution with Association Equation of State. *Ind. Eng. Chem. Res.* **2010**, *49* (15), 7085.
(25) González Prieto, M.; Sánchez, F. A.; Pereda, S. Thermodynamic Model for Biomass Processing in Pressure Intensified Technologies. *J. Supercrit. Fluids* **2015**, *96*, 53.
(26) Espinosa, S.; Bottini, S. B.; Brignole, E. A. Process Analysis and Phase Equilibria for the Removal of Chemicals from Fatty Oils Using Near-Critical Solvents. *Ind. Eng. Chem. Res.* **2000**, *39*, 3024.
(27) Espinosa, S.; Fornari, T.; Bottini, S. B.; Brignole, E. A. Phase Equilibria in Mixtures of Fatty Oils and Derivatives with near Critical Fluids Using the GC-EOS Model. *J. Supercrit. Fluids* **2002**, *23* (2), 91.
(28) Ferreira, O.; Macedo, E. A.; Brignole, E. A. Application of the GCA-EoS Model to the Supercritical Processing of Fatty Oil Derivatives. *J. Food Eng.* **2005**, *70* (4), 579.
(29) Andreatta, A. E.; Bottini, S. B.; Florusse, L. J.; Peters, C. J. Phase Equilibria of Allyl Sulfide+carbon Dioxide Binary Mixtures. *J. Supercrit. Fluids* **2006**, *38* (3), 306.
(30) Gañán, N. A.; Brignole, E. A. Supercritical Carbon Dioxide Fractionation of T. Minuta and S. Officinalis Essential Oils: Experiments and Process Analysis. *J. Supercrit. Fluids* **2013**, *78*, 12.
(31) Hegel, P. E.; Mabe, G. D. B.; Pereda, S.; Zabaloy, M. S.; Brignole, E. A. Phase Equilibria of near Critical CO2+propane Mixtures with Fixed Oils in the LV, LL and LLV Region. *J. Supercrit. Fluids* **2006**, *37* (3), 316.
(32) Soria, T. M.; González Prieto, M.; Pereda, S.; Bottini, S. B. Thermodynamic Modeling of Ethanol/gasoline Blends. In *25th European Symposium on Applied Thermodynamics*; Institute of Macromolecular Compounds, Russian Academy of Sciences: Saint Petersburg, Russia, 2011; p 25.
(33) Soria, T. M. Termodinámica En Biorefinerías: Producción de Bioetanol Y Alconaftas, Universidad Nacional del Sur, 2012.
(34) González Prieto, M.; Sánchez, F. A.; Pereda, S. Thermodynamic Modeling of Modern Fuels. In *X Iberoamerican Conference on Phase Equilibria and Fluid Properties for Process Design (EQUIFASE 2015)*; Universidad de Alicante: Alicante, 2015.
(35) Skjold-jørgensen, S. Group Contribution Equation of State (GC-EOS): A Predictive Method for Phase Equilibrium Computations over Wide Ranges of Temperature and Pressures up to 30 MPa. *Ind. Eng. Chem. Res.* **1988**, *27* (1), 110.
(36) Espinosa, S.; Foco, G. M.; Fornari, T. Revision and Extension of the Group Contribution Equation of State to New Solvent Groups and Higher Molecular Weight Alkanes. *Fluid Phase Equilib.* **2000**, *172*, 129.
(37) Cismondi, M.; Mollerup, J.; Brignole, E. A.; Zabaloy, M. S. Modeling the High-Pressure Phase Equilibria of Carbon Dioxide−triglyceride Systems: A Parameterization Strategy. *Fluid Phase Equilib.* **2009**, *281* (1), 40.
(38) Carnahan, N. F.; Starling, K. E. Equation of State for Nonattracting Rigid Spheres. *J. Chem. Phys.* **1969**, *51* (2), 635.
(39) Mansoori, G. A.; Leland, T. W., Jr. Statistical Thermodynamics of Mixtures. A New Version for the Theory of Conformal Solution. *J. Chem. Soc., Faraday Trans. 2* **1972**, *68*, 320.
(40) Renon, H.; Prausnitz, J. M. Local Compositions in Thermodynamic Excess Functions for Liquid Mixtures. *AIChE J.* **1968**, *14* (1), 135.
(41) Fredenslund, Å.; Gmehling, J.; Rasmussen, P. Vapor-Liquid Equilibria Using UNIFAC. A Group Contribution Method; Elsevier Ltd.: Amsterdam, 1977.
(42) Abrams, D. S.; Prausnitz, J. M. Statistical Thermodynamics of Liquid Mixtures: A New Expression for the Excess Gibbs Energy of Partly or Completely Miscible Systems. *AIChE J.* **1975**, *21* (1), 116.
(43) Chapman, W. G.; Gubbins, K. E.; Jackson, G.; Radosz, M. SAFT: Equation-of-State Solution Model for Associating Fluids. *Fluid Phase Equilib.* **1989**, *52*, 31.
(44) DIPPR801-Database. *Thermophysical Properties Database*; New York, 1998.
(45) Olds, R. H.; Reamer, H. H.; Sage, B. H.; Lacey, W. N. Phase Equilibria in Hydrocarbon Systems. The N-Butane-Carbon Dioxide System. *Ind. Eng. Chem.* **1949**, *41* (3), 475.
(46) Reamer, H. H.; Sage, B. H. Phase Equilibria in Hydrocarbon Systems. Volumetric and Phase Behavior of the N-Decane-CO2 System. *J. Chem. Eng. Data* **1963**, *8* (4), 508.
(47) Hottovy, J. D.; Luks, K. D.; Kohn, J. P. Three-Phase Liquid-Liquid-Vapor Equilibria Behavior of Certain Binary CO2-N-Paraffin Systems. *J. Chem. Eng. Data* **1981**, *26* (3), 256.
(48) Enick, R.; Holder, G. D.; Morsi, B. I. Critical and Three Phase Behavior in the Carbon Dioxide/tridecane System. *Fluid Phase Equilib.* **1985**, *22*, 209.
(49) Reamer, H. H.; Sage, B. H.; Lacey, W. N. Phase Equilibria in Hydrocarbon Systems. Volumetric and Phase Behavior of the Propane-Carbon Dioxide System. *Ind. Eng. Chem.* **1951**, *43* (11), 2515.
(50) Niesen, V. G.; Rainwater, J. C. Critical Locus, (vapor + Liquid) Equilibria, and Coexisting Densities (carbon Dioxide + Propane) at Temperatures from 311 K to 361 K. *J. Chem. Thermodyn.* **1990**, *22*, 777.
(51) Hamam, S. E. M.; Lu, B. C.-Y. Isothermal Vapor-Liquid Equilibria in Binary System Propane-Carbon Dioxide. *J. Chem. Eng. Data* **1976**, *21* (2), 200.
(52) Yucelen, B.; Kidnay, A. J. Vapor - Liquid Equilibria in the Nitrogen + Carbon Dioxide + Propane System from 240 to 330 K at Pressures to 15 MPa. *J. Chem. Eng. Data* **1999**, *44* (5), 926.
(53) Leu, A.-D.; Robinson, D. B. Equilibrium Phase Properties of the N-Butane-Carbon Dioxide and Isobutane-Carbon Dioxide Binary Systems. *J. Chem. Eng. Data* **1987**, *32* (4), 444.
(54) Hsu, J. J.-C.; Nagarajan, N.; Robinson, R. L. Equilibrium Phase Compositions, Phase Densities, and Interfacial Tensions for CO2 + Hydrocarbon Systems. 1. CO2 + N-Butane. *J. Chem. Eng. Data* **1985**, *30* (4), 485.
(55) Kalra, H.; Krishnana, T. R.; Robinson, D. B. Equilibrium-Phase Properties of Carbon Dioxide-N-Butane and Nitrogen-Hydrogen Sulfide Systems at Subambient Temperatures. *J. Chem. Eng. Data* **1976**, *21* (2), 222.
(56) Weber, L. A. Vapour-Liquid Equilibria Measurements for Carbon Dioxide with Normal and Isobutane from 250 to 280 K. *Cryogenics* **1985**, *25* (6), 338.
(57) Pozo de Fernández, M. E.; Zollweg, J. A.; Streett, W. B. Vapor-Liquid EquiWrium in the Binary System Carbon Dioxide + N-Butane. *J. Chem. Eng. Data* **1989**, *34* (3), 324.
(58) Shibata, S. K.; Sandler, S. I. High-Pressure Vapor-Liquid Equilibria Involving Mixtures of Nitrogen, Carbon Dioxide, and N-Butane. *J. Chem. Eng. Data* **1989**, *34* (3), 291.
(59) Weber, L. A. Simple Apparatus for Vapor-Liquid Equilibrium Measurements with Data for the Binary Systems of Carbon Dioxide with N-Butane and Isobutane. *J. Chem. Eng. Data* **1989**, *34* (2), 171.

DOI: 10.1021/acs.iecr.5b03269
Ind. Eng. Chem. Res. 2015, 54, 12415−12427

(60) Besserer, G. J.; Robinson, D. B. Equilibrium-Phase Properties of N-Pentane-Carbon Dioxide System. *J. Chem. Eng. Data* **1973**, *18* (4), 416.
(61) Leu, A.-D.; Robinson, R. L. Equilibrium Phase Properties of Selected Carbon Dioxide Binary Systems: N-Pentane-Carbon Dioxide and Isopentane-Carbon Dioxide. *J. Chem. Eng. Data* **1987**, *32* (4), 447.
(62) Tochigi, K.; Hasegawa, K.; Asano, N.; Kojima, K. Vapor - Liquid Equilibria for the Carbon Dioxide + Pentane and Carbon Dioxide + Toluene Systems. *J. Chem. Eng. Data* **1998**, *43* (6), 954.
(63) Li, Y.-H.; Dillard, K. H.; Robinson, R. L. Vapor-Liquid Phase Equilibrium for Carbon Dioxide-N-Hexane at 40, 80, and 120 °C. *J. Chem. Eng. Data* **1981**, *26* (1), 53.
(64) Wagner, Z.; Wichterle, I. High-Pressure Vapour—liquid Equilibrium in Systems Containing Carbon Dioxide, 1-Hexene, and N-Hexane. *Fluid Phase Equilib.* **1987**, *33* (1−2), 109.
(65) Kaminishi, G.-I.; Yokoyama, C.; Shinji, T. Vapor Pressures of Binary Mixtures of Carbon Dioxide with Benzene, N-Hexane and Cyclohexane up to 7 MPa. *Fluid Phase Equilib.* **1987**, *34* (1), 83.
(66) Kalra, H.; Kubota, H.; Robinson, D. B.; Ng, H.-J. Equilibrium Phase Properties of the Carbon Dioxide-N-Heptane System. *J. Chem. Eng. Data* **1978**, *23* (4), 317.
(67) Mutelet, F.; Vitu, S.; Privat, R.; Jaubert, J.-N. Solubility of CO2 in Branched Alkanes in Order to Extend the PPR78 Model (predictive 1978, Peng−Robinson EOS with Temperature-Dependent Kij Calculated through a Group Contribution Method) to Such Systems. *Fluid Phase Equilib.* **2005**, *238* (2), 157.
(68) Jiménez-Gallegos, R.; Galicia-Luna, L. A.; Elizalde-Solis, O. Experimental Vapor - Liquid Equilibria for the Carbon Dioxide + Octane and Carbon Dioxide + Decane Systems. *J. Chem. Eng. Data* **2006**, *51* (5), 1624.
(69) Weng, W.-L.; Chen, J.-T.; Lee, M.-J. High-Pressure Vapor-Liquid Equilibria for Mixtures Containing a Supercritical Fluid. *Ind. Eng. Chem. Res.* **1994**, *33* (8), 1955.
(70) Camacho-Camacho, L. E.; Galicia-Luna, L. A.; Elizalde-Solis, O.; Martínez-Ramírez, Z. New Isothermal Vapor−liquid Equilibria for the CO2+n-Nonane, and CO2+n-Undecane Systems. *Fluid Phase Equilib.* **2007**, *259* (1), 45.
(71) Jennings, D. W.; Schucker, R. C. Comparison of High-Pressure Vapor - Liquid Equilibria of Mixtures of CO 2 or Propane with Nonane and C 9 Alkylbenzenes. *J. Chem. Eng. Data* **1996**, *41* (4), 831.
(72) Sebastian, H. M.; Simnick, J. J.; Lin, H.-M.; Chao, K.-C. Vapor-Liquid Equilibrium in Binary Mixtures of Carbon Dioxide N-Decane and Carbon Dioxide + N-Hexadecane. *J. Chem. Eng. Data* **1980**, *25* (2), 138.
(73) Nagarajan, N.; Robinson, R. L., Jr. Equilibrium Phase Compositions, Phase Densities, and Interfacial Tensions for CO2 Hydrocarbon Systems. 2. CO2 + N-Decane. *J. Chem. Eng. Data* **1986**, *31* (2), 168.
(74) Chou, G. F.; Forbert, R. R.; Prausnitz, J. M. High-Pressure Vapor-Liquid Equilibria for CO2/n-Decane, CO2/Tetralin, and CO2/n-Decane/Tetralin at 71.1 and 104.4 °C. *J. Chem. Eng. Data* **1990**, *35* (1), 26.
(75) Shaver, R. D.; Robinson, R. L.; Gasem, K. A. M. An Automated Apparatus for Equilibrium Phase Compositions, Densities, and Interfacial Tensions: Data for Carbon Dioxide + Decane. *Fluid Phase Equilib.* **2001**, *179* (1−2), 43.
(76) Tsuji, T.; Tanaka, S.; Hiaki, T.; Saito, R. Measurements of Bubble Point Pressure for CO2 + Decane and CO2 + Lubricating Oil. *Fluid Phase Equilib.* **2004**, *219* (1), 87.
(77) Gardeler, H.; Fischer, K.; Gmehling, J. Experimental Determination of Vapor−Liquid Equilibrium Data for Asymmetric Systems. *Ind. Eng. Chem. Res.* **2002**, *41* (5), 1051.
(78) Nieuwoudt, I.; du Rand, M. Measurement of Phase Equilibria of Supercritical Carbon Dioxide and Paraffins. *J. Supercrit. Fluids* **2002**, *22* (3), 185.
(79) Henni, A.; Jaffer, S.; Mather, A. E. Solubility of N_2O and CO_2 in N-Dodecane. *Can. J. Chem. Eng.* **1996**, *74* (4), 554.
(80) Wang, L.-S.; Lang, Z.-X.; Guo, T.-M. Measurement and Correlation of the Diffusion Coefficients of Carbon Dioxide in Liquid Hydrocarbons under Elevated Pressure. *Fluid Phase Equilib.* **1996**, *117*, 364.
(81) Secuianu, C.; Feroiu, V.; Geană, D. Phase Equilibria of Carbon dioxide + 1-Nonanol System at High Pressures. *J. Supercrit. Fluids* **2010**, *55* (2), 653.
(82) Secuianu, C.; Feroiu, V.; Geană, D. Investigation of Phase Equilibria in the Ternary System Carbon dioxide+1-Heptanol+n-Pentadecane. *Fluid Phase Equilib.* **2007**, *261* (1−2), 337.
(83) Schwarz, B. J.; Prausnitz, J. M. Solubilities of Methane, Ethane, and Carbon Dioxide in Heavy Fossil-Fuel Fractions. *Ind. Eng. Chem. Res.* **1987**, *26* (11), 2360.
(84) Gasem, K. A. M.; Dickson, K. B.; Dulcamara, P. B.; Nagarajan; Robinson, R. L., Jr. Equilibrium Phase Compositions, Phase Densities, and Interfacial Tensions for CO2 + Hydrocarbon Systems. 5. CO2 + N-Tetradecane. *J. Chem. Eng. Data* **1989**, *34* (2), 191.
(85) Tanaka, H.; Yamaki, Y.; Kato, M. Solubility of Carbon Dioxide in Pentadecane, Hexadecane, and Pentadecane + Hexadecane. *J. Chem. Eng. Data* **1993**, *38* (3), 386.
(86) Spee, M.; Schneider, G. M. Fluid Phase Equilibrium Studies on Binary and Ternary Mixtures of Carbon Dioxide with Hexadecane, 1-Dodecanol, 1,8-Octanediol and Dotriacontane at 393.2 K and at Pressures up to 100 MPa. *Fluid Phase Equilib.* **1991**, *65*, 263.
(87) Kordikowski, A.; Schneider, G. M. Fluid Phase Equilibria of Binary and Ternary Mixtures of Supercritical Carbon Dioxide with Low-Volatility Organic Subtances up to 100 MPa and 393 K: Cosolvency Effects and Miscibility Windows. *Fluid Phase Equilib.* **1993**, *90*, 149.
(88) Brunner, G.; Teich, J.; Dohrn, R. Phase Equilibria in Systems Containing Hydrogen, Carbon Dioxide, Water and Hydrocarbons. *Fluid Phase Equilib.* **1994**, *100*, 253.
(89) D'Souza, R.; Patrick, J. R.; Teja, A. S. High Pressure Phase Equilibria in the Carbon Dioxide - N-Hexadecane and Carbon Dioxide—water Systems. *Can. J. Chem. Eng.* **1988**, *66*, 319.
(90) Pöhler, H.; Scheidgen, A. L.; Schneider, G. M. Fluid Phase Equilibria of Binary and Ternary Mixtures of Supercritical Carbon Dioxide with a 1-Alkanol and an N-Alkane up to 100 MPa and 393 K—cosolvency Effect and Miscibility Windows (Part II). *Fluid Phase Equilib.* **1996**, *115* (1−2), 165.
(91) Fall, D.; Fall, J.; Luks, K. Liquid-Liquid-Vapor Immiscibility Limits in Carbon Dioxide+ N-Paraffin Mixtures. *J. Chem. Eng. Data* **1985**, *30*, 82.
(92) Elbaccouch, M. M.; Bondar, V. I.; Carbonell, R. G.; Grant, C. S. Phase Equilibrium Behavior of the Binary Systems CO2 + Nonadecane and CO2 + Soysolv and the Ternary System CO2 + Soysolv + Quaternary Ammonium Chloride Surfactant. *J. Chem. Eng. Data* **2003**, *48* (6), 1401.
(93) Sato, Y.; Tagashira, Y.; Maruyama, D.; Takishima, S.; Masuoka, H. Solubility of Carbon Dioxide in Eicosane, Docosane, Tetracosane, and Octacosane at Temperatures from 323 to 473 K and Pressures up to 40 MPa. *Fluid Phase Equilib.* **1998**, *147* (1−2), 181.
(94) Gasem, K. a. M.; Robinson, R. L. Solubilities of Carbon Dioxide in Heavy Normal Paraffins (C20-C44) at Pressures to 9.6 MPa and Temperatures from 323 to 423 K. *J. Chem. Eng. Data* **1985**, *30* (1), 53.
(95) Huie, N. C.; Luks, K. D.; Kohn, J. P. Phase-Equilibria Behavior of Systems Carbon Dioxide-N-Eicosane and Carbon Dioxide-N-Decane-N-Eicosane. *J. Chem. Eng. Data* **1973**, *18* (3), 311.
(96) Feng, G.; Mather, A. Solubility of Hydrogen Sulfide in N-Eicosane at Elevated Pressure. *J. Chem. Eng. Data* **1992**, *37* (4), 412.
(97) Fall, D. J.; Luks, K. D. Phase Equilibria Behavior of the Systems Carbon Dioxide + N-Dotriacontane and Carbon Dioxide + N-Docosane. *J. Chem. Eng. Data* **1984**, *29* (4), 413.
(98) Tsai, F.-N.; Yau, J.-S. Solubility of Carbon Dioxide in N-Tetracosane and in N-Dotriacontane. *J. Chem. Eng. Data* **1990**, *35* (1), 43.
(99) Huang, S. H.; Lin, H.-M.; Chao, K.-C. Carbon Dioxide, Methane, and Ethane in N-Octacosane. *J. Chem. Eng. Data* **1988**, *33* (2), 143.
(100) Hottovy, J. D.; Kohn, J. P.; Luks, K. D. Partial Miscibility Behavior of the Ternary Systems Methane−Propane−n-Octane,

DOI: 10.1021/acs.iecr.5b03269
Ind. Eng. Chem. Res. 2015, 54, 12415−12427

Methane−n-Butane−n-Octane, and Methane−Carbon Dioxide−n-Octane. *J. Chem. Eng. Data* **1982**, *27* (3), 298.
(101) Kulkarni, A. A.; Zarah, B. Y.; Luks, K. D.; Kohn, J. P. Phase-Equilibria Behavior of System Carbon Dioxide-N-Decane at Low Temperatures. *J. Chem. Eng. Data* **1974**, *19* (1), 92.
(102) Van der Steen, J.; de Loos, T. W.; de Swaan Arons, J. The Volumetric Analysis and Prediction of Liquid-Liquid-Vapor Equilibria in Certain Carbon-Dioxide + N-Alkane Systems. *Fluid Phase Equilib.* **1989**, *51*, 353.
(103) Cismondi, M.; Michelsen, M. L. Global Phase Equilibrium Calculations: Critical Lines, Critical End Points and Liquid−liquid−vapour Equilibrium in Binary Mixtures. *J. Supercrit. Fluids* **2007**, *39* (3), 287.
(104) Cismondi Duarte, M.; Gaitán, M. *Global Phase Equilibrium Calculations (GPEC)*; Phasety—Thermodynamics Software and Consulting in Industries for the Oil and Chemical: Córdoba, Argentina, 2008.
(105) Miller, M. M.; Luks, K. D. Observations on the Multiphase Equilibria Behavior of Corrich and Ethane-Rich Mixtures. *Fluid Phase Equilib.* **1989**, *44*, 295.
(106) Poettmann, F. H.; Katz, D. L. Phase Behavior of Binary Carbon Dioxide-Paraffin Systems. *Ind. Eng. Chem.* **1945**, *37*, 847.
(107) Choi, E.; Yeo, S. Critical Properties for Carbon Dioxide + N-Alkane Mixtures Using a Variable-Volume View Cell. *J. Chem. Eng. Data* **1998**, *43* (5), 714.
(108) Liu, J.; Qin, Z.; Wang, G.; Hou, X.; Wang, J. Critical Properties of Binary and Ternary Mixtures of Hexane + Methanol, Hexane + Carbon Dioxide, Methanol + Carbon Dioxide, and Hexane + Carbon Dioxide + Methanol. *J. Chem. Eng. Data* **2003**, *48* (6), 1610.
(109) Chester, T. L.; Haynes, B. S. Estimation of Pressure-Temperature Critical Loci of CO2 Binary Mixtures with Methyl-Tert-Butyl Ether, Ethyl Acetate, Methyl-Ethyl Ketone, Dioxane and Decane. *J. Supercrit. Fluids* **1997**, *11*, 15.
(110) Fall, D. J.; Luks, K. D. Liquid-Liquid-Vapor Phase Equiltbria of the Binary System Carbon Dioxide + N-Tridecane. *J. Chem. Eng. Data* **1985**, *30* (3), 276.
(111) Scheidgen, A. L. Fluidphasengleichgewichte Binären Und Ternären Kohlendioxidmischungen Mit Schwerfüchtigen Organischen Substanzen Bis 100 MPa, Universität Bochum, 1997.
(112) Pando, C.; Renuncio, J. A. R.; Christensen, J. J.; Izatt, R. M. The Excess Enthalpies of (carbon Dioxide + Pentane) at 308.15 and 323.15 K from 7.58 to 12.45 MPa. *J. Chem. Thermodyn.* **1983**, *15*, 259.
(113) Zúñiga-Moreno, A.; Galicia-Luna, L. A.; Camacho-Camacho, L. E. Compressed Liquid Densities and Excess Volumes of CO2 + Decane Mixtures from (313 to 363) K and Pressures up to 25 MPa. *J. Chem. Eng. Data* **2005**, *50* (3), 1030.
(114) Besserer, G. J.; Robinson, D. B. Equilibrium-Phase Properties of I-Butane-Carbon Dioxide. *J. Chem. Eng. Data* **1973**, *18* (3), 298.
(115) Besserer, G. J.; Robinson, D. B. Equilibrium-Phase Properties of Isopentane-Carbon Dioxide System. *J. Chem. Eng. Data* **1975**, *20* (1), 93.
(116) Buxing, H.; Haike, Y.; Riheng, H. Solubiliiy of CO2 in a Mixed Solvent of N-Octane and I-Octane at Elevated Pressures. *Thermochim. Acta* **1990**, *169*, 217.
(117) Zhang, J. S.; Lee, S.; Lee, J. W. Solubility of CO2, N2, and CO2 + N2 Gas Mixtures in Isooctane. *J. Chem. Eng. Data* **2008**, *53* (6), 1321.
(118) Prausnitz, J. M.; Benson, P. R. Solubility of Liquids in Compressed Hydrogen, Nitrogen, and Carbon Dioxide. *AIChE J.* **1959**, *5* (2), 161.
(119) Zamudio, M.; Schwarz, C. E.; Knoetze, J. H. Phase Equilibria of Branched Isomers of C10-Alcohols and C10-Alkanes in Supercritical Carbon Dioxide. *J. Supercrit. Fluids* **2011**, *59*, 14.

DOI: 10.1021/acs.iecr.5b03269
Ind. Eng. Chem. Res. 2015, 54, 12415−12427